24th INTERNATIONAL CONGRESS ON SOUND AND VIBRATION
23–27 July 2017, London

SOMMERFELD EFFECT AND CRITICAL BEHAVIOUR OF A NON-IDEAL ASYMMETRIC SYSTEM

Eung-Soo Shin

Chungbuk National University, School of Mechanical Engineering, Cheongju, Chungbuk, Korea
email: esshin@chungbuk.ac.kr

Kee-Sung Kim

Chungbuk National University, School of Mechanical Engineering, Cheongju, Chungbuk, Korea,

This work intends to investigate the effect of the rotor asymmetry on the critical behaviour of a non-ideal system. The analytic equations of motion are derived and then a parameter study is performed with variation of the rotor asymmetry, the external and internal damping and the motor voltage. Results show that the critical behaviour can be categorized into four classes from the viewpoints of the whirling stability and passage through resonance. A slight asymmetry has a positive effect on the passage through resonance but a large asymmetry has the opposite effect. Also, the analytic results are in a good agreement with numerical simulation unless the rotor asymmetry is large.

Keywords: non-ideal system, Sommerfeld phenomena, asymmetry, critical behaviour, stability

1. Introduction

It is well known that the whirling motion of non-ideal systems is strongly affected by the dynamics of a power unit [1]. Many works have been performed for investigating the dynamic characteristics including the whirling stability [2], critical behaviour around resonance [3, 4] and so-called Sommerfeld phenomena [5, 6].

In this work, a non-ideal system with an asymmetric rotor is considered and an analytic and numerical approaches are employed to investigate the effect of asymmetry on the stability and critical behaviour through resonance.

2. Analytic formulation

2.1 Equations of motion for a non-ideal asymmetric system

As shown in Fig. 1, the non-ideal system in this work consists of a massless asymmetric shaft, a rotor with mass eccentricity and a DC motor. The equations of motion for the shaft whirling can be derived with respect to the rotating ξ_r–η_r coordinate system as

$$\ddot{\xi} + 2\{\zeta_E + \zeta_I(1+\beta)\}\dot{\xi} - 2\Omega\dot{\eta} + \{(1+\alpha) - \Omega^2\}\xi - 2\zeta_E\Omega\eta = \Omega^2\cos\lambda \tag{1}$$

$$\ddot{\eta} + 2\{\zeta_E + \zeta_I(1-\beta)\}\dot{\eta} + 2\Omega\dot{\xi} + \{(1-\alpha) + \Omega^2\}\xi + 2\zeta_E\Omega\xi = \Omega^2\sin\lambda \tag{2}$$

Above, ξ and η are non-dimensionalized by the radius of eccentricity and all the differentiations are taken for a dimensionless time $\tau = \omega_0 t$. Also, all the parameters are dimensionless such that

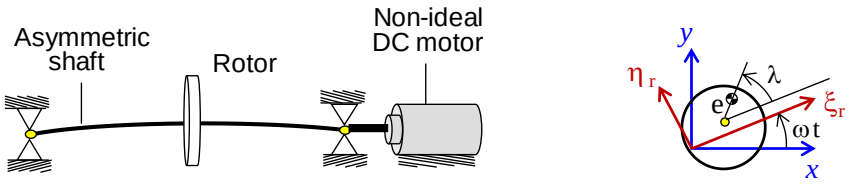

(a) Schematic (b) Mass-eccentric rotor

Figure 1: A non-ideal system with the shaft asymmetry.

$$k = \frac{k_\xi + k_\eta}{2};\ \omega_0 = \sqrt{\frac{k}{m}};\ \Omega = \frac{\omega}{\omega_0};\ \alpha = \frac{k_\xi - k_\eta}{k_\xi + k_\eta};\ \beta = \frac{c_{I\xi} - c_{I\eta}}{c_{I\xi} + c_{I\eta}};\ \zeta_E = \frac{c_E}{2\sqrt{mk}};\ \zeta_I = \frac{c_{I\xi} + c_{I\eta}}{4\sqrt{mk}} \quad (3)$$

For the non-ideal system, the motor speed is affected by the whirling motion of the shaft as well as the motor torque. Or,

$$\dot{\Omega} + \zeta_m \Omega = (V - \zeta_b \Omega) - \frac{\zeta_I}{J_m}\left[(1-\beta)\dot{\eta}\xi - (1-\beta)\dot{\xi}\eta\right] \quad (4)$$

All the parameters in Eq. (4) are also dimensionless, where J_m is the motor's mass moment of inertia, ζ_m is the motor damping, ζ_b is the motor's back-emf constant and V is the motor voltage. As shown in the right hand side of Eq. (4), the excitation torque on the motor is generated by two sources: the first is from the motor and the second is from the non-conservative circulatory forces due to the rotating internal damping of the shaft.

2.2 Sommerfeld phenomena

In case of stable whirling, the power supplied by the motor should be balanced by the power dissipated by mechanical circulatory motion along the whirling orbit. From Eq. (4), the supplied power can be expressed in a non-dimensional form as

$$P_S = \Omega\,(V - \zeta_b \Omega) \quad (5)$$

On the other hand, the power is dissipated through the external and internal damping of the shaft and the motor damping. Or,

$$P_D = \left(\frac{4A_S^2}{J_m}\right)\Omega^2\left[\zeta_E + \zeta_I(1 - \beta\cos 2\phi)\right] + \zeta_m \Omega^2 \quad (6)$$

In Eq. (6), A_S is the steady-state amplitude of whirling and ϕ is the phase angle of the steady-state response from the ξ axis. By imposing the power balance between P_S and P_D, the following condition is derived:

$$4A_S^2\left[\zeta_E + \zeta_I(1 - \beta\cos 2\phi)\right]\Omega = J_m\left[V - (\zeta_m + \zeta_b)\Omega\right] \quad (7)$$

Meanwhile, the shaft response can also be obtained by solving Eqs. (1) and (2). Since ξ and η are both constant at steady-state, the whirling amplitude A_S is given as

$$A_S = \frac{\Omega^2\sqrt{(1-\Omega^2)^2+(2\zeta_E\Omega)^2-\alpha^2-2\alpha(1-\Omega^2)\cos 2\lambda-4\alpha\zeta_E\Omega\sin 2\lambda}}{(1-\Omega^2)^2+(2\zeta_E\Omega)^2-\alpha^2} \tag{8}$$

Solving Eqs. (7) and (8) simultaneously, A_S can be obtained as a function of V. When multiple solutions for A_S exist for a single value of V, the Sommerfeld phenomena occur and a sudden change in the motor speed and the whirling amplitude is observed.

2.3 Whirling stability

For the system governed by Eqs. (1) and (2), the whirling stability can be determined by the characteristic equation as follows. By assuming that $\xi(t)=\xi_0 e^{i\omega_0 st}$ and $\eta(t)=\eta_0 e^{i\omega_0 st}$, the characteristic equation is derived as

$$\begin{aligned} &s^4+4s^3(\zeta_E+\zeta_I)+2s^2\left\{1+\Omega^2+2(\zeta_E+\zeta_I)^2-2\beta\zeta_I^2\right\} \\ &\quad+4s\left\{\zeta_E(1+\Omega^2)+\zeta_I(1-\Omega^2-\alpha\beta)\right\}+(1-\Omega^2)^2-\alpha^2+4\Omega^2\zeta_E^2=0 \end{aligned} \tag{9}$$

A positive real part of roots, which is given in terms of the rotation speed and the external and internal damping, means that the system is unstable. Since the Sommerfeld phenomena cause an abrupt change in the rotation speed, they are closely related to the whirling stability. Thus, the characteristics of the Sommerfeld phenomena should be investigated with consideration for the whirling stability.

3. Sommerfeld phenomena in a non-ideal asymmetric system

3.1 Overview

In this work, a parametric study is performed to estimate the fundamental characteristics of the Sommerfeld phenomena for the system in Fig. 1. The parameters includes the shaft asymmetry α, the motor power V, the shaft damping ζ_E and ζ_I. The parameter β is not independently considered but related to α under the assumption that the shaft is uniform.

$$\beta=\frac{1-\sqrt{1-\alpha^2}}{\alpha}, \qquad \text{where } 0<\alpha<1 \tag{10}$$

Analytic results are first obtained from the power balance in Eqs. (7) and (8) and then numerically validated by integrating Eqs. (1) through (3). Table 1 shows a summary of system constants.

Table 1: System constants

Description (symbol)	Constants (unit)	Description (symbol)	Constants
Rotor mass (m)	1 (kg)	Motor inertia (J_m)	500
Rotor stiffness (k)	2.25 x 10^4 (N/m)	Motor damping (ζ_m)	1.33x10^{-4}
Mass eccentricity (e)	2 x 10^{-3} (m)	Motor back-emf (ζ_b)	3 x 10^{-3}

3.2 Fundamental characteristics of the Sommerfeld phenomena

Figures 2 and 3 show results about the motor speed and the whirling amplitude for α=0.1 and 0.3, respectively, while ζ_E=0.2 and ζ_I=0.1. In both cases, jump-ups in the motor speed are observed and

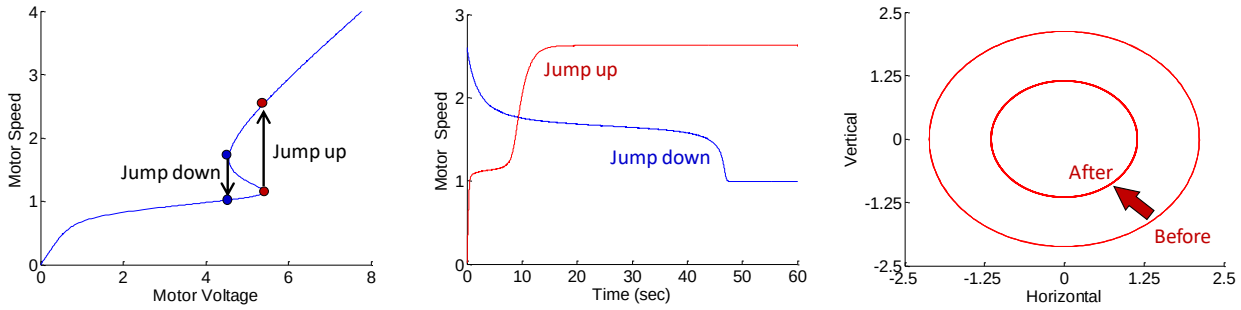

(a) Jump-up/down vs. power (b) Motor speed (c) Whirling amplitude

Figure 2: Sommerfeld phenomena (α=0.1).

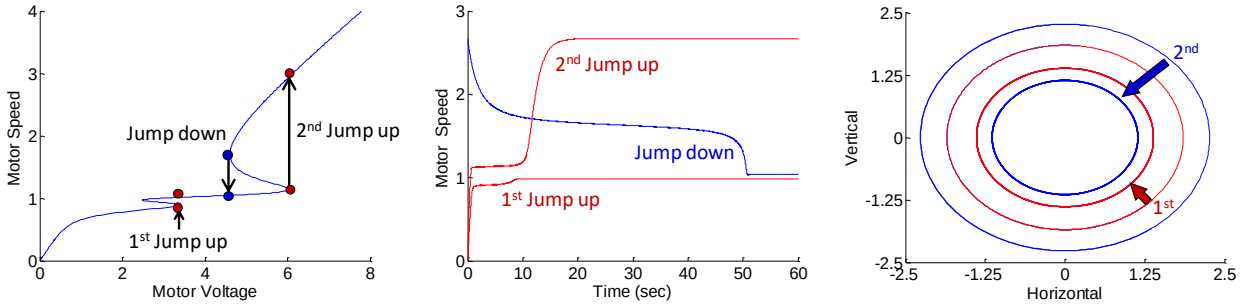

(a) Jump-up/down vs. power (b) Motor speed (c) Whirling amplitude

Figure 3: Sommerfeld phenomena (α=0.3).

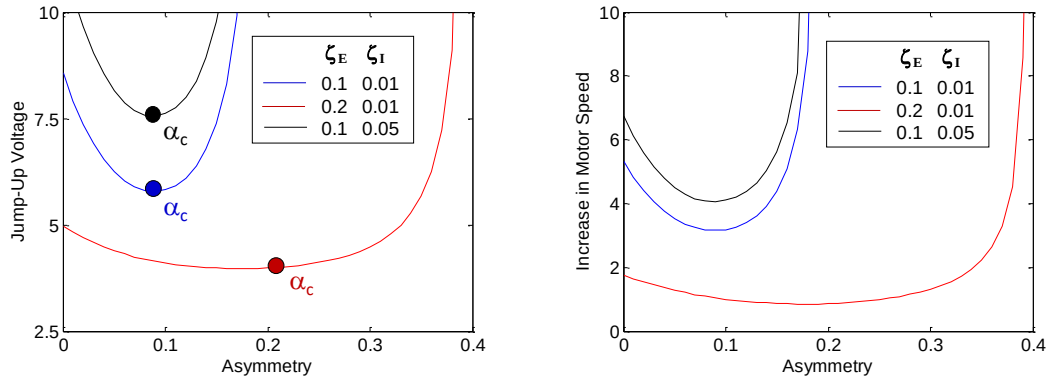

(a) Motor power (b) Motor speed

Figure 4: Effects of asymmetry on the Sommerfeld phenomena at the jump-up.

the system remains stable after jump-ups. As α increases, however, the Sommerfeld phenomena become complicated such that a two-stage jump-up may occur.

Figure 4 demonstrates a combined effect of the asymmetry and the damping on the motor and shaft behavior at the jump-up. When $\alpha < \alpha_c$, the shaft asymmetry helps jump up through resonance with a less motor power regardless of the damping. On the other hand, the asymmetry has the opposite effect in case that $\alpha < \alpha_c$.

The external damping has a positive effect on jumping regardless of the asymmetry, but the internal damping has a negative effect. Also, the motor power at the jump-up is more significantly influenced by the external damping than the internal damping.

3.3 Numerical validation

In order to verify the analytic results based on the steady-state power balance, Eqs. (1), (2) and (3) are numerically integrated and transient responses during the jump-up are obtained. Figure 5 shows the analytic and numerical results of the motor power versus the shaft asymmetry. In case that α is small, the analytical results well match the numerical. For a large value of α, however, the difference between the analytic and numerical results also increases. As α increases, the possibility of the unstable whirling becomes higher, which means that steady-state conditions cannot be achieved and the analytic results may not be accurate. Figure 6 illustrates a stability diagram with variation of the shaft asymmetry and the internal damping. Two types of instability exist: the first is the primary resonance and the second is the supercritical instability. The shaft asymmetry has a more significant effect on the instability around primary resonance.

4. Critical behaviour through resonance

4.1 Stability diagram

The critical behaviour of a non-ideal system can be classified from the viewpoint of the Sommerfeld phenomena and the whirling stability. Table 2 shows a brief summary of the classification.

In Class I, the motor power is not sufficient to jump up out of resonance and the system remains stable in a subcritical region. In Class II, the system becomes unstable due to the primary resonance. Both the shaft whirling and the motor speed fluctuates with a large amplitude. In Class III, the system jumps up through resonance to a supercritical condition and the motor speed remains below the stability limit, which can be approximated as $1+(\zeta_E/\zeta_I)$. In Class IV, the motor speed exceeds the stability boundary in the supercritical region and a large fluctuation in the whirling amplitude is caused.

Figure 7 shows stability diagrams between the shaft asymmetry and the motor power with variation of the internal damping. As the shaft asymmetry increases, the Class II region expands rapidly regardless of the motor power and the internal damping. Also, the Class IV region grows as the internal damping increases.

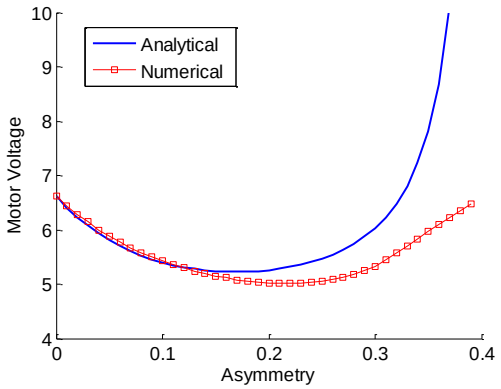

Figure 5: Comparison of the jump-up voltage.

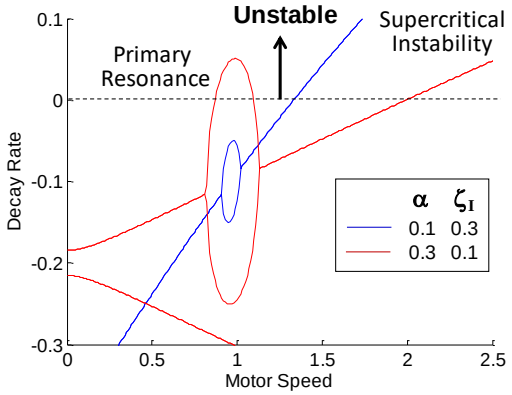

Figure 6: Stability vs. motor speed.

Table 2: Classification of the critical behaviour

Class	Passage through resonance	Whirling Stability	Descriptions
I	No	Yes	Motor power not enough to jump up
II	No	No	Primary resonance
III	Yes	Yes	Jump up below the stability limit
IV	Yes	No	Supercritical instability

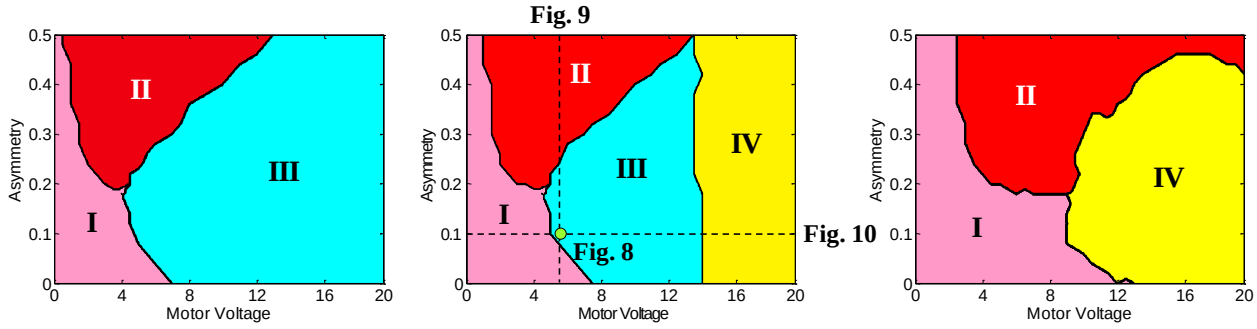

(a) ζ_I=0.0 (b) ζ_I=0.01 (c) ζ_I=0.1

Figure 7: Diagrams of the critical behaviour with respect to the asymmetry and power (ζ_E=0.1).

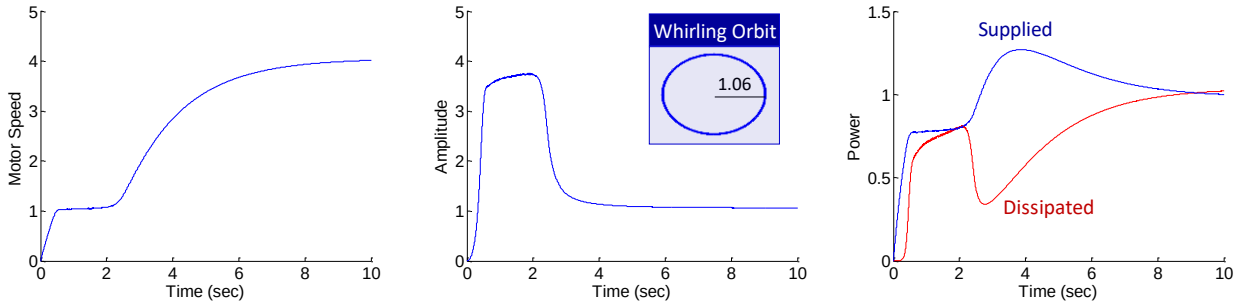

(a) Motor speed (b) Whirling amplitude (c) Power balance

Figure 8: Critical behaviour through resonance (ζ_E=0.1; ζ_I=0.1; V=5.5).

4.2 Effects of system parameters on the critical behaviour

Numerical simulation are performed to obtain the transient results of the motor speed, the whirling amplitude and the power balance. Figure 8 displays the typical characteristics of Class III near a stability boundary with α equal to 0.1. A stable jump-up in the motor speed occurs and the whirling reaches a steady-state condition with a perfect balance between the supplied and dissipated power.

If α increases within the Class III region, there is slight variation in the whirling but the jump-up occurs more smoothly as shown in the case α=0.2 of Fig. 9(a). As α further increases to enter the Class II region, the system becomes unstable and both the motor speed and the shaft whirling experience the large amplitude motion as in the case α=0.3 of Figs. 9(a) and (b).

Also, the motor power has a significant effect on the critical behavior as shown in Fig. 10. As V increases, the system demonstrates various characteristics from the stable subcritical motion of Class I to the unstable supercritical motion of Class IV. When V=10, a smooth coast-up is observed in the motor speed without the Sommerfeld phenomena. If V further increases to 16, the system experiences the supercritical instability of Class IV. A large variation in the dissipated power is observed as shown in Fig. 10(b).

Although the whirling is unstable in both Class II and Class IV, the transient whirling responses are different from each other as shown in Fig. 11. Also, the motor speed in Class II varies with a large amplitude as in Fig. 9(a) but it reaches a steady-state after jump-up in Class IV.

5. Conclusions

The critical behaviour of a non-ideal asymmetric rotor is investigated by an analytic approach based on the equations of motion and the parameter study with variation of the rotor asymmetry, the motor power and the external and internal damping. Results show that the critical behaviour can be

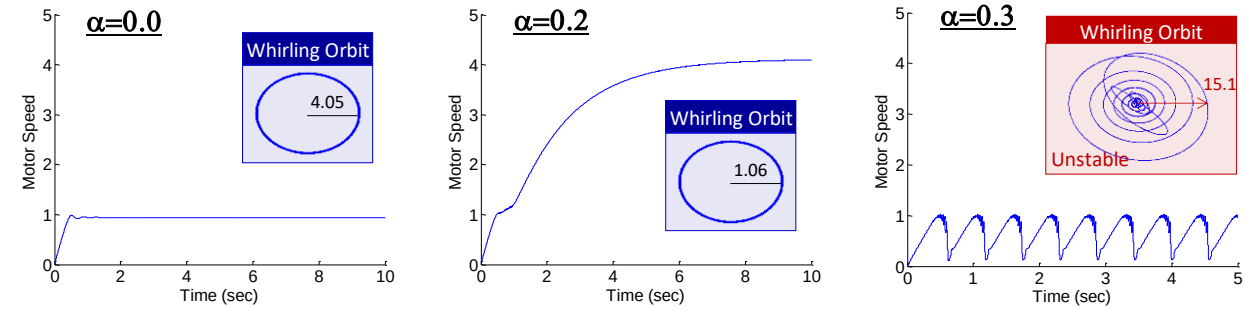

(a) Motor speed

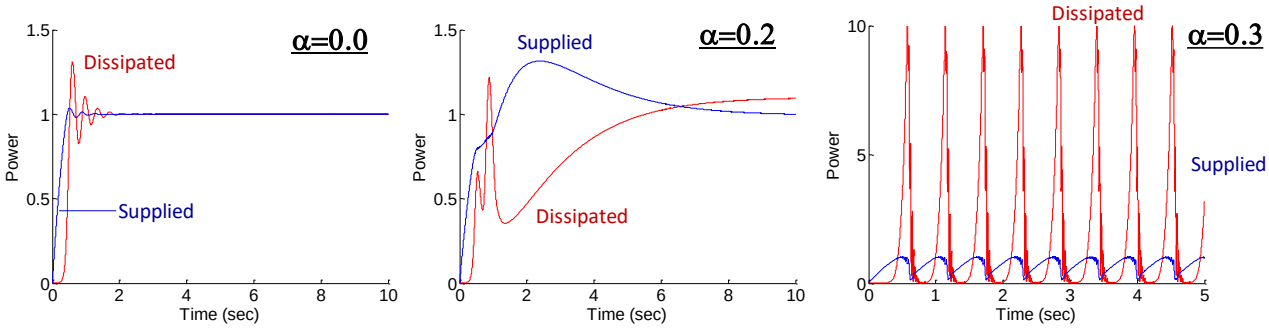

(b) Power balance

Figure 9: Effect of the asymmetry on the critical behaviour (ζ_E=0.1; ζ_I=0.1; V=5.5).

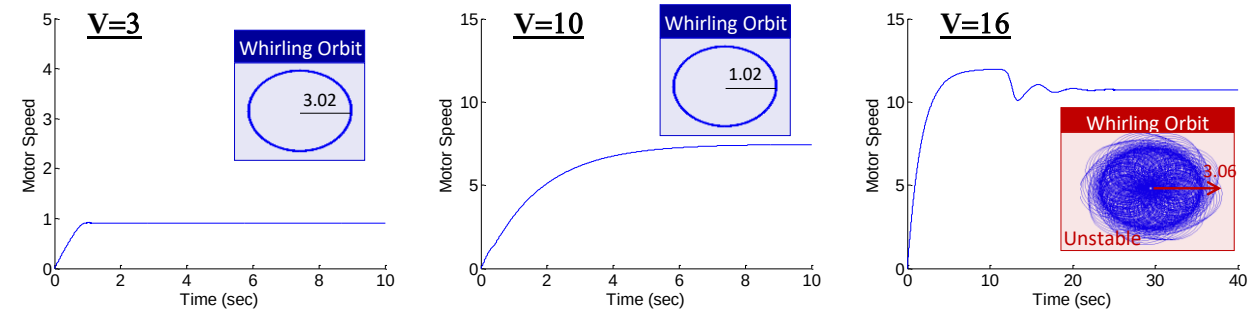

(a) Motor speed

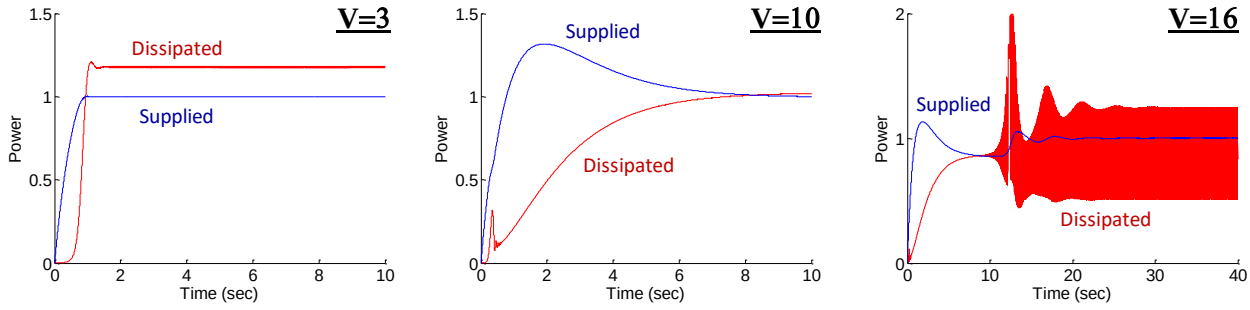

(b) Power balance

Figure 10: Effect of the motor power on the critical behaviour (ζ_E=0.1; ζ_I=0.1; α=0.1).

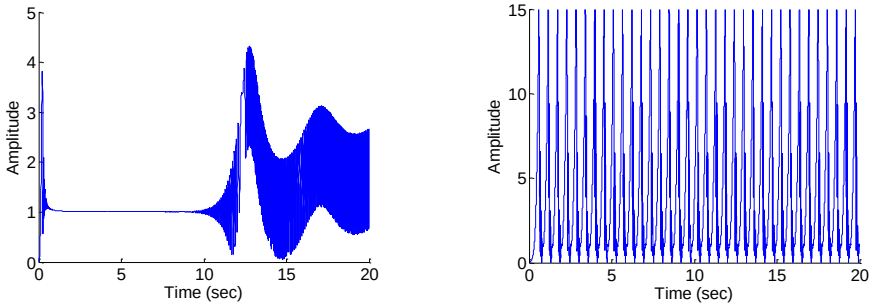

(a) Primary resonance (b) Rotating internal damping

Figure 11: Unstable whirling.

categorized into four classes from the viewpoints of the whirling stability and passage through resonance. A slight asymmetry has a positive effect on the passage through resonance but a large asymmetry has the opposite effect. The external damping helps jump up through resonance regardless of the asymmetry. Furthermore, the external damping has a more significant effects on the motor power at the jump-up than the internal damping.

Also, the analytic results are in a good agreement with numerical simulation unless the rotor asymmetry is large.

REFERENCES

1 Cveticanin, L. Dynamics of the non-ideal mechanical systems: A review, *Journal of Serbian Society for Computational Mechanics*, **4** (2), 55–86, (2010).

2 Dasgupta, S. S., Samantaray, A. K. and Bhattacharyya, R. Stability of an internally damped non-flexible spinning shaft, *International Journal of Non-Linear Mechanics*, **15**, 286–293, (2010).

3 Fradkov, A., Tomchina, O., and Tomchin, D. Controlled passage through resonance in mechanical systems, *Journal of Sound and Vibration*, **330**, 1065–1073, (2011).

4 Verichev, N. N. Chaotic torsional vibration of imbalanced shaft driven by a limited power supply, *Journal of Sound and Vibration*, **331**, 384–393, (2012).

5 Karthikeyan, M., Bisoi, A., Samantaray, A. K. and Bhattacharyya, R. Sommerfeld effect characterization in rotors with non-ideal drive from ideal drive response and power balance, *Mechanism and Machine Theory*, **91**, 269–288, (2015).

6 Shin, E. S. Sommerfeld phenomena of an asymmetric rotor, *Journal of Korean Society of Manufacturing Technology Engineers*, **23** (1), 56–63, (2014).